

A Mathematical Model for Predicting the Carbon Sequestration Potential
of Exposed Ordinary Portland Cement (OPC) Concrete

by

ADRIANA SOUTO MARTINEZ

M.Arch., ETSAB, Polytechnic University of Catalonia, 2013

A thesis submitted to the
Faculty of the Graduate School of the
University of Colorado in partial fulfillment
of the requirement for the degree of
Master of Science
Architectural Engineering

2017

This thesis entitled:

A Mathematical Model for Predicting the Carbon Sequestration Potential of Exposed
Ordinary Portland Cement (OPC) Concrete

written by Adriana Souto Martínez

has been approved for the Civil Environmental and Architectural Engineering Department

Prof. Wil V. Srubar III

Prof. Gregor Henze

Prof. Yunping Xi

Date _____

The final copy of this thesis has been examined by the signatories, and we find that both the content and the form meet acceptable presentation standards of scholarly work in the above mentioned discipline.

Souto Martinez, Adriana (M.S., Architectural Engineering)

A Mathematical Model for Predicting the Carbon Sequestration Potential of Exposed Ordinary Portland Cement (OPC) Concrete

Thesis directed by Associate Professor Wil V. Srubar III

This study concerns the development of a simple mathematical model that calculates the theoretical carbon sequestration potential of exposed ordinary portland cement (OPC) concrete. OPC concrete sequesters non-trivial amounts of carbon dioxide (CO_2) via carbonation – a chemical reaction between cement paste and atmospheric CO_2 . Formulated by the reaction chemistries of cement hydration and carbonation, the model accounts for cement type and content, exposure, time, and type and quantity of supplementary cementitious materials (SCMs). Once validated with data from literature, the model is implemented to investigate the effect of these factors and the influence of compressive strength and geometry, namely surface-area-to-volume (SA/V) ratio, on total carbon sequestration (kg CO_2) of exposed concrete elements. Results demonstrate that (a) low tetracalcium aluminoferrite (C_4AF) cements, (b) compressive strength, (c) high CO_2 exposure, (d) no SCMs, (e) time, (f) high SA/V ratios, and (g) indoor environments enhance the in situ carbon sequestration of exposed OPC concrete.

ACKNOWLEDGEMENTS

I would first like to thank my thesis advisor, Dr. Wil V. Srubar III, who consistently guided and supported me through this research. Without his help and passionate participation and input, this work could not have been successfully conducted.

I would also like to thank Professor Gregor Henze and Professor Yunping Xi for serving on my defense committee. I am grateful for their very valuable comments on this thesis.

I would also like to acknowledge the Department of Civil, Environmental and Architectural Engineering, the College of Engineering and Applied Sciences, the Balsells fellowship, and the Sustainable Infrastructure Materials Laboratory (SIMLab) at the University of Colorado Boulder for making this research possible.

Finally, I must express my very profound gratitude to my family and friends for their unfailing support and unwavering encouragement throughout my years of study, especially to my mum, who has always inspired me and pushed me to be my best. This accomplishment would not have been possible without you.

Thank you.

CONTENTS

Chapter 1	1
1.1 Purpose of the Study	1
1.2 Scope of the Study	1
1.2.1 Phase I: Mathematical model development	1
1.2.2 Phase II: Model implementation	2
Chapter 2	3
2.1 Environmental impacts of buildings	3
2.2 Environmental impacts of concrete	3
2.3 Concrete carbonation	5
Chapter 3	9
3.1 Theoretical formulation	9
3.1.1 Cement mineral content	9
3.1.2 Cement hydration reactions	10
3.1.3 Pozzolanic reaction	11
3.1.4 Carbonation reaction	11
3.1.5 Carbon sequestration potential	12
3.1.6 Carbonation depth	14
3.1.7 Carbonated volume	16
3.1.8 Total mass of sequestered CO ₂	17
3.2 Model validation	17
Chapter 4	19
4.1 Concrete Column case study	19
4.1.2 Effect of cement type	19
4.1.3 Effect of concrete compressive strength	22
4.1.4 Effect of SCMs	29
4.1.5 Effect of environmental exposure	30
4.1.6 Effect of structural geometry	33
Chapter 5	38
References	41

LIST OF TABLES

Table 1 Average chemical and mineral composition of cement types by weight according to ASTM C150. Oxides and minerals are presented in cement chemistry notation.	10
Table 2 Carbon sequestration potential coefficients per cement type and SCM	14
Table 3 Parameters values for k_1 and n based on exposure classification	15
Table 4 Carbonation environmental exposure classifications	16
Table 5 OPC concrete element case studies and parameters used for model validation	18
Table 6 Sample mixture proportions for concretes of varying compressive strengths.	23
Table 7 Column geometries considered in analyzing the effect of SA/V on carbon sequestration potential.....	33

LIST OF FIGURES

Figure 1 Effect of cement type on carbon sequestration potential in (a) XC1 high- (800 ppm) and (b) XC4 low-concentration (300 ppm) CO ₂ environments after 25, 50, 75, 100, 125, and 150 years of exposure for a 40 MPa concrete column.....	21
Figure 2 Effect of compressive strength on carbon sequestration potential in (a) XC1 high- (800 ppm) and (b) XC4 low-concentration (300 ppm) CO ₂ environments after 25, 50, 75, 100, 125, and 150 years of exposure for a Type I cement concrete.	25
Figure 3 Effect of cement type, namely (a) Type I, (b) Type II, (c) Type III, (d) Type IV, (e) Type V, and (f) White, and time on the carbon sequestration potential of 15 MPa, 30 MPa, and 45 MPa compressive strength concrete columns.....	28
Figure 4 Anticipated reductions in carbon sequestration potential, per SCM type and weight-percent cement replacement.	30
Figure 5 Effect of CO ₂ concentration and exposure environment, namely (a) XC1, (b) XC2, (c) XC3, and (d) XC4, on the carbon sequestration of a 40 MPa Type I, Type II, Type III, Type IV, Type V, and White cement concrete columns	32
Figure 6 Influence of SA/V ratio on sequesterable CO ₂ for Type I, 40 MPa structural concrete columns in (a) high and (b) low-concentration CO ₂ environments after 25, 50, 75, 100, 125, and 150 years.	35

CHAPTER 1

INTRODUCTION

1.1 Purpose of the Study

The purpose of the study is: (a) to develop a mathematical model that calculates the theoretical carbon sequestration potential of exposed ordinary portland cement (OPC) concrete; (b) to implement the model to investigate the effect of cement type and content, compressive strength, exposure, time, type, quantity of supplementary cementitious materials (SCMs) and geometry (namely surface-area-to-volume ratio) on total carbon sequestration.

1.2 Scope of the Study

The research completed within the scope of the study is organized into two phases to accomplish the twofold purpose outlined in Section 1.1. Phase I addresses the development of a mathematical model to predict carbon sequestration of OPC concrete. Phase II addresses part (b) the implementation of model in two case study examples to investigate the effect of each parameter involved in the equations.

1.2.1 Phase I: Mathematical model development

The mathematical model developed is based on the hydration reaction and carbonation chemistries of Ordinary Portland Cement (OPC). In formulating the model, average mineral contents for six different types of OPC were linked to the carbon sequestration potential of the expected type and amount of hydration products. Anticipated reductions in carbonation potential due to the type and amount of SCMs were also incorporated. The resulting model directly

calculates total anticipated carbon sequestration potential (kg CO₂) from eight input variables, namely (1) total concrete volume, (2) total exposed concrete surface area, (3) cement type, (4) cement content per unit mass of concrete, (5) SCM type, (6) percent-replacement of cement with SCMs, (7) CO₂ exposure classification, and (8) time. The model is validated using data reported in the literature and implemented herein to demonstrate the effect of these variables, as well as the effect of concrete compressive strength and surface-area-to-volume (SA/V) ratio, on the carbon sequestration potential of exposed OPC concrete elements.

The mathematical model is described in detail in chapter 3, where cement mineral content compositions are provided together with explanations of cement hydration formulations and pozzolanic (SCMs) and carbonation reaction mechanisms. In addition, since total carbon sequestration depends on carbonation depth, a model developed by the Portuguese National Laboratory [Monteiro 2012] is presented and utilized in this thesis. Finally, the study provides a discussion on concrete carbonation degree and the final total carbon sequestration model is derived.

1.2.2 Phase II: Model implementation

The validated model is subsequently implemented in a concrete column case study example, where the effect of cement type, compressive strength, type and quantity of SCMs, environmental exposure, and structural geometry is analyzed. A discussion on each of these analysis is provided in Chapter 4.

CHAPTER 2

BACKGROUND AND MOTIVATION

2.1 Environmental impacts of buildings

Buildings are a primary consumer of energy and emitter of greenhouse gases. Buildings are responsible for approximately 40% of total energy consumption and 40% of carbon dioxide (CO₂) emissions in the United States and Europe [Barnett 2007, U.S. DOE 2008]. Worldwide, buildings demand approximately a third of all primary energy during their life cycle: from construction to demolition. Several studies found that the operational energy consumption during the use phase of a building contributes largely to total environmental impacts (80-90%) [Ramesh 2010; Asif 2007]. However, net-zero energy buildings strive to reduce operational impacts using advanced building envelope technologies and on-site renewable energy generation, which, in turn, effectively increases the percentage of impacts associated with physical materials and components. In the most extreme case, the environmental impacts associated with completely passive buildings are 100% attributable to material manufacture, transportation, and construction [Simonen 2014]. In recognition that the impacts of common materials, like cement and concrete, and components are of growing concern, numerous studies that quantify the environmental impacts of common construction materials are common in the literature [Bribián 2010].

2.2 Environmental impacts of concrete

Portland cement concrete is the most commonly utilized construction material on earth [Crow 2008] and the second most consumed material after water. It contains approximately 15% cement, which manufacture is the main contributor of greenhouse gas emissions, and 80%

aggregates [Mehta 2001]. In addition, concrete also consumes large amounts of fresh water: around 1 trillion liters every year are used only during concrete mixing [Mehta 2001].

The widespread production, use, and disposal of OPC impart global environmental consequences that contribute to greenhouse gas emissions, global warming, and climate change. 1.6 billion tonnes of cement are produced every year [Mehta 2001], and 5-8% of total global carbon dioxide (CO₂) emissions are consequence of its manufacture [Worrell 2001]. Approximately 50% of the CO₂ emissions associated with OPC manufacture is attributable to a chemical reaction, namely calcination of calcium carbonate (CaCO₃) [Huntzinger 2009], a predominant mineral in limestone and the primary raw material in OPC. Calcination is achieved by heating CaCO₃ in a kiln to temperatures in excess of 1000°C, resulting in calcium oxide (CaO) and gaseous CO₂. In addition to chemical calcination, approximately 40% of the CO₂ emissions in OPC manufacture is attributable to indirect emissions that occur via the combustion of fossil fuels to heat the kiln for the calcination and cement clinkering reactions to occur. Electricity used to power additional machinery and the transportation of cement account for the remaining 10%. When producing one ton of OPC, approximately 4 GJ of energy are used, and 1 ton of CO₂ is released to the atmosphere.

Numerous experimental studies have identified strategies and best practices to reduce the environmental impacts of OPC Concrete. Such strategies include incorporation of recycled aggregates and mineral fillers, such as ground limestone. The environmental impacts of recycled aggregate concrete vs. natural aggregate concrete are largely discussed in the literature, [Marinkovic 2010; Knoeri 2013]. Others have investigated the effect of minimizing total OPC

content in concrete by partially replacing OPC with supplementary cementitious materials (SCMs) [Malhotra 1999; Berndt 2008]. SCMs are a waste or by-product generated by other industrial processes that, if not used as binders, would be landfilled. These by-products are silica-rich elements, such as slag (SL), silica fume (SF), metakaolin (MK), or fly ash (FA) that, through a pozzolanic reaction, contribute to enhance concrete properties such as long-term strength, permeability or workability [Yang 2015]. According to Damtoft, et al., (2008), global CO₂ emissions related to cement manufacture could be reduced by 17% if all the available fly ash and slag was used as a replacement. However, while total reductions might be achieved, the use of SCMs also decreases the amount of CO₂ that concrete elements can potentially sequester while in service. The model presented in this thesis accounts for these reductions in concrete carbonation when using SCMs.

2.3 Concrete carbonation

The process of carbonation is a chemical reaction that primarily occurs between calcium hydroxide in hydrated cement and atmospheric carbon dioxide (CO₂), resulting in calcium carbonate. While concrete carbonation is usually associated with rebar corrosion, it is a carbon sequestration process with a positive environmental benefit. The carbonation process is described in detail in Chapter 3.

Previous research has addressed the mechanism of carbonation [Roy 1999; Peter 2008; Galan 2010; Torgal 2012; Ashraf 2016], and several models have been developed to predict carbonation depths in concrete. Initially, these models were obtained as a tool to estimate durability and time to steel-reinforced corrosion. Most of these prediction models are based on standard reaction engineering tools. For instance, Papadakis, et al., (1990) provided with

different analytical expressions corresponding to different environmental situations. The authors found that for a relative humidity in excess of 50%, the carbonation depth presents a sharp carbonation front and thus, a simple model can be used to predict it. However, at lower RH, the mechanism of carbonation need to account for the effect of the aqueous film thickness, and thus another model was provided.

Jiang, et al., (2000) developed a mathematical model to predict carbonation depth of concretes with high amounts of Fly Ash. They compared the model with accelerated carbonation tests to demonstrate that cement content and water to binder ratio are the main factors that drive carbonation depth.

Steffens, et al., (2002), published a paper where a theoretical model to predict carbonation of concrete structures was developed. This model was based on reaction kinetics: the movement and retention of heat, moisture and carbon dioxide based on diffusion law equations. The model was developed using finite element concepts and numerical time integration techniques. This model was also verified using results from experimental tests from the literature.

Wang, et al., (2009) also studied how Fly Ash affected carbonation. Their numerical model was based on two models: hydration and carbonation. They obtained the amount of product in the mixture susceptible to carbonate and the porosity of the material as a function of curing age. With this, the diffusivity of CO in concrete was obtained, and therefore a formula to determine carbonation depth. Only fly ash was studied, but they claimed similarities with other pozzolanic elements made this model suitable for other blended materials.

Monteiro, et al., (2012), conducted a statistical study to improve the current carbonation models based on Fick's first law and carbonation coefficients, K , which depend on environmental conditions. These conditions were better evaluated by analyzing 100 existing structures up to 99 years old. With these analyses, they defined correlations between carbonation coefficients and factors such as age, effect of painting, compressive strength or exposure conditions. Due to the simplicity, but at the same time completeness of these analyses, this model is used in the formulation of the mathematical model proposed in this study.

Finally, Kashef-Haghighi, et al., (2015) used partial differential equations to describe gas transport, dissolution in concrete pore water and reaction with components present in cement to predict CO_2 uptake. They determined that the specific surface area of the compounds in the reaction defines uptake rate and extent, and that the key reactions are related to the C_3S present in the cement. In addition, the authors found that carbonation rate is controlled by the partial pressure of CO_2 .

While these models emerged out of durability concerns of steel-reinforced concrete, a few recent studies have attempted to account for the amount of CO_2 sequestered during the service life of OPC concrete structures [Pomer 2006; Lagerblad 2006; Pade 2007; Nilsson 2009; Collins 2010; Lee 2013; García-Segura 2014; Yang 2014]. For example, Pade and Guimaraes (2007), estimated CO_2 uptake due to carbonation over 100 years and compared it to the amount of CO_2 emitted during OPC manufacture. Collins (2010), included CO_2 capture in a lifecycle assessment (LCA) of structural and crushed reinforced concrete. García-Segura (2014), studied the

consequences of using blended cements in terms of enhanced durability and reductions in carbon sequestration. In addition, García-Segura, et al., (2014) and Yepes, et al., (2015) integrated estimates of sequestered carbon within a structural optimization framework to simultaneously consider cost and carbon emission in the design of prestressed concrete highway girders. Despite notable advances, however, these existing models exhibit complexities or limitations, including a limited capability to accommodate any cement or SCM type, which restricts their generalizability and implementation in practice.

Aside from these studies, only the negative impacts of OPC concrete (i.e., limestone calcination) are included when quantifying the environmental impacts of concrete elements, and the carbon sequestration potential of reinforced concrete is, at present, largely neglected in the accounting.

To help architects and engineers quantify these environmental impacts, whole-building lifecycle assessment (WBLCA) has emerged as a tool that can be utilized during the design phase of buildings. Numerous examples of WBLCA implementation case studies can be found in the literature [Peuportier 2001; Junnila 2003, Haapio 2008; Bribián 2009; Basbagill 2013; Khasreen 2009]. The majority of these studies focus on comparing embodied versus operational energy by assuming a standard service life of 50, 60 or 75 years. Building service life and in-situ materials durability predictions remain a current challenge of WBLCA implementation, not only in estimating total energy consumption, but also in determining building maintenance and refurbishment needs. In most cases, if durability is not considered when quantifying the cradle-to-grave environmental impacts of buildings, results may lead to misinformed decision-making [Srubar 2014]. Similarly, incorporating durability and carbon sequestration potential into WBLCA frameworks would ultimately improve the accuracy of the environmental accounting.

CHAPTER 3

MATHEMATICAL MODEL

3.1 Theoretical formulation

To calculate total sequesterable CO₂ for an exposed concrete element, first, the type of cement in the concrete mixture is mathematically linked to the theoretical type and amount of hydration reaction products, including calcium hydroxide (CH), also known as portlandite, which is essential for the carbonation reaction.

Next, the amount of CH is mathematically adjusted based on the type and amount of SCMs present in the concrete mixture. Total sequesterable CO₂ per mass of carbonated cement paste is then calculated based on the stoichiometry of the carbonation reaction. Given the geometry of a concrete element (namely surface area and volume), length of time, and CO₂ exposure, total volume of carbonated concrete is calculated using a well-accepted predictive model for carbonation depth. Total volume of carbonated cement paste in the carbonated concrete is estimated using the known cement content per unit volume of concrete (kg/m³), which is obtainable from concrete mixture proportions. From these calculations, total sequesterable CO₂ (kg CO₂) for a specific concrete element can be computed. Explicit mathematical details of the model formulation are presented in the following sections.

3.1.1 Cement mineral content

Table 1 lists the average chemical composition and mineral content for the main classifications of OPC as specified by ASTM C150 and White cement [American society of Testing and Materias, 2016]. Primary oxides present in OPC, including silicon dioxide (S), aluminum oxide

(A), ferric oxide (F), calcium oxide (C), magnesium oxide (M), sulfur trioxide (Š), and sodium oxide (N), comprise four main cement minerals, including tricalcium silicate (C₃S), dicalcium silicate (C₂S), tricalcium aluminate (C₃A) and tetracalcium aluminoferrite (C₄AF). Tailored mineral compositions enhance desired properties in the fresh- and hardened states, such as early strength, durability, or aesthetics in the case of White cement.

Table 1 Average chemical and mineral composition of cement types by weight according to ASTM C150. Oxides and minerals are presented in cement chemistry notation.

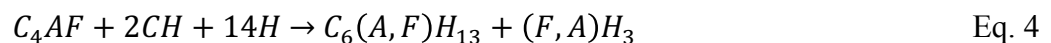
Cement Type	Average Oxide Composition (%)								Average Mineral (Bogue) Composition (%)				
	S (SiO ₂)	A (Al ₂ O ₃)	F (Fe ₂ O ₃)	C (CaO)	M (MgO)	Š (SO ₃)	N (Na ₂ O)	Other	C ₃ S	C ₂ S	C ₃ A	C ₄ AF	Oth
I	20.5	5.4	2.6	63.9	2.1	3.0	0.61	1.9	54	18	10	8	10
II	21.2	4.6	3.5	63.8	2.1	2.7	0.51	1.6	55	19	6	11	9
III	20.6	4.9	2.8	63.4	2.2	3.5	0.56	2.0	55	17	9	8	11
IV	22.2	4.6	5.0	62.5	1.9	2.2	0.36	1.2	42	32	4	15	7
V	21.9	3.9	4.2	63.8	2.2	2.3	0.48	1.2	54	22	4	13	7
White	22.7	4.1	0.3	66.7	0.9	2.7	0.18	2.4	63	18	10	1	8

3.1.2 Cement hydration reactions

The primary hydration reactions of tricalcium silicate (C₃S) and dicalcium silicate (C₂S) with water (H) produce both a calcium silicate hydrate (C₃S₂H₈) phase and CH as follows:



The primary hydration reactions of other cement minerals, namely tricalcium aluminate (C₃A) and tetracalcium aluminoferrite (C₄AF) yields:



where, in cement chemistry notation, CŠH₂ is gypsum, C₆AŠ₃H₃₂ is ettringite, C₆(A,F)H₁₃ is calcium aluminoferrite hydrate and (F,A)H₃ is aluminoferrite hydrate, respectively.

3.1.3 Pozzolanic reaction

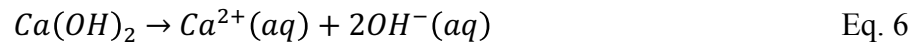
The addition of siliceous SCMs effectively reduces the carbon sequestration potential of hydrated portland cement by reacting with available CH to produce CSH according to the following reaction:



Therefore, the total amount of available CH in a given concrete mixture must be mathematically adjusted based on the type and amount of SCM in the concrete mixture (see Section 3.1.5).

3.1.4 Carbonation reaction

The process of carbonation is a chemical reaction that occurs primarily between readily available CH and atmospheric CO₂ that precipitates calcite, the most stable polymorph of calcium carbonate, CaCO₃. In conventional chemistry notation, the reactions are as follows:



While trace amounts of magnesium and sodium are present in cement, the precipitation of other alkali and alkaline carbonate salts via similar carbonation reactions is not thermodynamically favored.

This formulation assumes, albeit conservatively, that only available CH participates in the carbon sequestration. Many research studies have highlighted the role of calcium silicate hydrate (CSH) in the carbonation process [Johannesson 2001]. In addition, the ferritic phases in cement paste

(e.g., AFt, AFm) have been shown to carbonate [Nishikawa 1992]. However, to preserve simplicity, these carbonation reactions have not been included in the mathematical formulation. The formulation also assumes that no carbonation occurs after CH depletion. However, further carbonation is likely due to the existence of calcium-containing compounds formed via the pozzolanic reaction (i.e., CSH). The assumption that only available CH participates in carbon sequestration, however, is conservative, in that the model will not produce overestimations of the net positive carbon, but rather err on the side of under prediction.

A negative impact of carbonation is that CO₂ gas, which initially dissolves in water to form carbonic acid, H₂CO₃, can subsequently react with alkalis in the pore solution (e.g., Ca²⁺). The depletion of hydroxide ions (OH⁻) from the pore solution chemistry effectively lowers the pH of the pore solution from approximately 12.5–9.0. This reduction can destabilize the protective passive oxide layer that initially forms on the surface of mild steel reinforcement. Destabilization of the passive layer can lead to reinforcement corrosion in the presence of sufficient oxygen and water. Therefore, sufficient cover depth is required to protect steel reinforcement, especially in severe exposure conditions. Alternative reinforcement strategies, such as the use of epoxy-coated rebar or glass fiber-reinforced polymer (GFRP) rebar, can increase the service-life of reinforced OPC concrete that may be prone to chemical deterioration via carbonation.

3.1.5 Carbon sequestration potential

From these equations, the theoretical amount of sequesterable CO₂ via the formation of calcium carbonate in the hydrated cement paste on a per mass basis can be computed according to the following equation:

$$C_m = \alpha - \beta \cdot y \quad \text{Eq. 8}$$

where carbon sequestration potential, C_m , is defined as the total mass percentage of sequesterable CO_2 per kg of carbonated cement paste (kg CO_2/kg cement) in the concrete and y is the percent replacement (by mass of cement) by SCMs in decimal form. Table 2 lists values for the coefficient α , which accounts for variation in cement type. Assuming a theoretical 100% hydration of cement minerals, $\phi_h = 1.0$, the α coefficient reported in Table 1 was obtained by the following equation:

$$\alpha = \phi_h MW_{CH} \left(\frac{3}{2} \cdot \frac{B_{C_3S}}{MW_{C_3S}} + \frac{1}{2} \cdot \frac{B_{C_2S}}{MW_{C_2S}} - \frac{2}{1} \cdot \frac{B_{C_4AF}}{MW_{C_4AF}} \right) \quad \text{Eq. 9}$$

where B_{C_3S} , B_{C_2S} , and B_{C_4AF} are the Bogue composition (%) of C_3S , C_2S , and C_4AF , respectively, and MW_{C_3S} , MW_{C_2S} , MW_{C_4AF} , and MW_{CH} are the molecular weights of C_3S (228.314 g/mol), C_2S (172.237 g/mol), C_4AF (485.955 g/mol), and CH (74.09 g/com). Multipliers (3/2), (1/2), and (2) are stoichiometric ratios of CH produced or consumed by C_3S , C_2S , and C_4AF , respectively, in the hydration reactions presented in Eq. 1, Eq. 2., and Eq. 4. The relative magnitudes of the parameter are quantitative measures of the amount of readily available CH that is produced by the hydration reactions.

To validate these predictions, similar calculations were obtained for total theoretical grams (g) of CH produced per gram of cement assuming 100% hydration. The results yield values of 0.28, 0.28, 0.23, and 0.27 kg CH per kg cement for cement Types I-V, respectively, which align well with the empirical and theoretical predictions of CH content as a function of hydration degree reported by Mounanga (2004).

The coefficient β accounts for the type and amount of SCMs. If the total silica content of the actual SCM is known, or can be obtained via laboratory analysis prior to mixture proportioning, the coefficient β can be computed according to the general equation:

$$\beta = 1.1 \cdot \sigma \quad \text{Eq. 10}$$

where σ is the weight percent (%) of silicon dioxide (SiO_2) in the SCM in decimal form. The scalar of 1.1 was derived by dividing the molar ratio of calcium hydroxide to silica shown Eq. 6 (3/2) by the molecular weight of silicon dioxide (60.083 g/mol) and multiplied by the molecular weight of CO_2 (44.01 g/mol), which yields a final scale factor of $1.09873 \approx 1.1$. If the total silica content is neither known nor obtainable, average silica contents for common types of SCM are listed in Table 2. However, it is cautioned that the utilization of average silica contents listed in Table 2 will impart uncertainty in the modeling prediction.

Table 2 Carbon sequestration potential coefficients per cement type and SCM

Cement Type	α	Supplementary Cementitious Material (SCM)	Average σ % SiO_2	β
Type I	0.165	Fly Ash (Class F)	50%	0.55
Type II	0.163	Fly Ash (Class C)	25%	0.27
Type III	0.166	Slag	35%	0.38
Type IV	0.135	Silica Fume	90%	0.99
Type V	0.161	Metakaolin	50%	0.55
White	0.203			

3.1.6 Carbonation depth

Accurately predicting carbonation depth after a period of prolonged exposure is difficult because the process is complex. The depth of the carbonation front is affected by moisture, temperature, CO_2 concentration, time, and, as discussed, type and amount of cement and SCMs, which dictates the availability of reactive CH.

Despite these challenges, an empirical model for predicting the carbonation depth, x (mm), has been proposed by the Portuguese National Laboratory [Monteiro 2012] and used by previous researchers:

$$x = \sqrt{\left(\frac{2 \cdot c \cdot t}{R}\right)} \cdot \left[\sqrt{k_0 k_1 k_2} \left(\frac{1}{t}\right)^n\right] \quad \text{Eq. 11}$$

where c is the environmental CO_2 concentration (kg/m^3) (Note: $1 \text{ kg}/\text{m}^3 \text{ CO}_2 = 516 \text{ ppb}$), t is exposure time (years), k_0 is equal to 3.0, k_2 is equal to 1.0 for standard curing, and R is the carbonation resistance coefficient ($\text{kg year}/\text{m}^5$) that is calculated for Type I and Type II cement according to:

$$R = 0.0016 \cdot f_c^{3.106} \quad \text{Eq. 12}$$

and for Types III-V and White cement according to:

$$R = 0.0018 \cdot f_c^{2.862} \quad \text{Eq. 13}$$

where f_c is the compressive strength (MPa). The factors k_1 and n , shown in Table 3, are dependent upon exposure classifications as outlined below in Table 4.

Table 3 Parameters values for k_1 and n based on exposure classification [Monteiro 2012]

Parameter	XC1	XC2	XC3	XC4
k_1	1.0	0.20	0.77	0.41
n	0	0.183	0.02	0.085

Table 4 Carbonation environmental exposure classifications [Monteiro 2012]

Class	Environment	Examples
XC1	Dry or permanently humid	Reinforced concrete inside buildings or structures, except areas of high humidity Reinforced concrete permanently under non-aggressive water
XC2	Humid, rarely dry	Reinforced concrete under non-aggressive soil Reinforced concrete subjected to long periods of contact with non-aggressive water
XC3	Moderately humid	Outer surfaces of reinforced concrete sheltered from wind-driven rain Reinforced concrete inside structures with moderate to high air humidity
XC4	Cyclically humid and dry	Reinforced concrete exposed to wetting/drying cycles Outer surfaces of reinforced concrete exposed to rain or outside the scope of XC2

3.1.7 Carbonated volume

To calculate total carbonated volume, first, the type of cement (Type I-V/White), design compressive strength, and mixture proportions, namely the total mass (kg) per unit volume (m^3) of concrete, of concrete must be known, as well as the initial exposed surface area, SA, and total volume of all structural and non-structural exposed concrete members. Exposed concrete includes concrete elements without coatings or paints that may inhibit ingress of CO_2 .

The total carbonated volume at any finite point in time can be calculated by multiplying the total carbonation depth, x , computed according to Eq. (11), by the total surface area of exposed concrete members:

$$V_c = SA \cdot x \quad \text{Eq. 14}$$

with the limitation that the total carbonated concrete volume, V_c , must be less than or equal to the total volume of OPC concrete, V . The theoretical limit of sequesterable CO_2 of a given volume of concrete after an infinite amount of time can be calculated by assuming $V_c = V$.

3.1.8 Total mass of sequestered CO₂

The total mass of sequesterable CO₂, C_s (kg CO₂), can be calculated by multiplying the total mass of carbonated cement paste by the carbon sequestration potential, C_m , calculated according to Eq. 8:

$$C_s = \phi_c C_m \cdot [V_c \cdot m] \quad \text{Eq. 15}$$

where ϕ_c is the degree of carbonation, m is the total mass of cement per unit volume of concrete (kg/m³) obtained from the concrete batch mixture proportions, and the quantity in brackets is equal to the total mass of carbonated cement paste. While a theoretical 100% degree of carbonation, $\phi_c = 1.0$, is assumed herein for model implementation and demonstration purposes, actual degrees of carbonation ranging from 0.40-0.72 have been experimentally obtained by previous researchers [Engelsen 2014; Fridh 2013; Van Ballen 2005; villain 2006; Thiery 2013]. Lower degrees of carbonation are more conservative, which will result in lower estimates of sequestered CO₂.

3.2 Model validation

Experimental data related to carbonation exist in the literature, yet the majority of studies focus on validation of predictive models for carbonation-induced corrosion. As previously discussed, only a few studies provide have used carbonation data to predict total sequestered CO₂ (kg CO₂) by concrete elements in situ. Some studies present specific examples used herein for comparison. Table 5 shows comparative values reported by those authors and those predicted by the model, along with the modeling parameters and assumptions (if any) that used for validation. The results substantiate that predicted values for total carbon sequestration of concrete elements align well with those reported by other studies. For example, according to results obtained by García-

Segura, et al., (2014) , a 0.3 Å~ 0.3 Å~ 3 m ($SA/V = 14 \text{ m}^{-1}$) Type I, 25 MPa concrete column sequesters up to 16.4 kg CO₂ after 100 years of exposure. The mathematical model presented herein predicts that the same Type I, 25 MPa concrete column with an identical geometry would theoretically sequester a maximum of approximately 17.0 kg CO₂, a difference of 3.7%. Similar results were obtained for the other case studies, establishing that the proposed generalized mathematical approach is a valid estimate of theoretical carbon sequestration potential in OPC and blended OPC cement concretes.

Table 5 OPC concrete element case studies and parameters used for model validation

Sample	Cement Type	Cement Content (kg/m ³)	Compressive Strength (MPa)	SCM Type	SCM Quantity (%)	(%)	Surface Area (m ²)	Volume (m ³)	Exposure Class	CO ₂ (ppm)	Time (years)	Reported (kg CO ₂)	Model Prediction (kg CO ₂)	Reference
1	Type I*	373	>35	Fly Ash (Class C*)	36	0.75	2.21	0.221	Outdoor Exposed	300	70	1.8	1.3	Pomer & Pade (2006)
2	Type I*	480	>35	-	-	0.75	2.00	0.017	Outdoor Exposed	300	50	0.9	1.0	Pomer & Pade (2006)
3	Type I*	349-463	24-35	Fly Ash (Class C*)	12.9-14.9	0.75-1.0*	14,400-17,800	11.743	Outdoor/Indoor	300-800*	20	91.5	50.2-110.6	Lee, et al. (2012)
4	Type I	250	25	-	-	0.75-1.0*	3.6	0.27	Outdoor/Indoor	300-800*	100	16.4	7.0-16.99	Garcia-Segura, et al. (2013)
5	Type II	250	25	Fly Ash (Class C*)	20	0.75-1.0*	3.6	0.27	Outdoor/Indoor	300-800*	100	11.4	2.35-11.63	Garcia-Segura, et al. (2013)
6	Type II	360	30	-	-	0.75	9.6	NS	Indoor	800*	50	36.4*	27.8	Lagerblad (2006)
7	Type I	277	NS	-	-	0.35	NS	NS	Indoor	800*	100	6.1	5.8	Nilsson & Fridh (2011)

CHAPTER 4

MODEL IMPLEMENTATION

4.1 Concrete Column case study

The model formulated in Chapter 3 was implemented to investigate the effect of time, cement type, and compressive strength, as well as the type and amount of SCMs on carbon sequestration potential of exposed concrete elements. In addition, the influence of exposure classification and structural geometry on the carbon sequestration potential of exposed OPC concrete elements was investigated herein.

4.1.2 Effect of cement type

Figure 1 shows the effect of cement type on carbon sequestration potential of a 0.5 x 0.5 x 3 meters ($SA/V = 8 \text{ m}^{-1}$) concrete column for all types of cement after 25, 50, 75, 100, 125 and 150 years in both an indoor environment (XC1) with a high concentration (800 ppm, $1.55 \times 10^{-3} \text{ kg/m}^3$) of CO_2 and an outdoor environment (XC4) with low concentration (300 ppm, $0.581 \times 10^{-3} \text{ kg/m}^3$) of CO_2 . A compressive strength of 40 MPa was assumed, and no SCMs were added to isolate the effect of cement type on carbon sequestration potential.

Expectedly, the total amount of sequestered CO_2 increases with both exposure time and favorable exposure conditions. For example, the Type I cement concrete column exhibits a 145% increase in sequesterable CO_2 between 25 and 150 years in a XC1 (high- CO_2) environment. A 289% increase is observed for the same Type I cement concrete column in a XC1 versus XC4 (low- CO_2) environment after 150 years of exposure. All cement types exhibit similar time- and exposure-dependent behaviors.

White cement concrete consistently sequesters more CO₂ than other cement types due to its inherently low C₄AF mineral composition. According to Eq. 4, hydration of C₄AF consumes CH, thus, low C₄AF would result in more CH available for CO₂ sequestration. Similarly, the Type III cement concrete exhibits the second-highest CO₂ sequestration potential, due to its lower C₄AF content compared to Type I, II, IV, and V cements (Table 1). Type I and Type II cement concretes exhibit similar behaviors in both CO₂ environments. This behavior is anticipated due to similarities in both chemical composition and carbonation resistance of Type I and Type II cements.

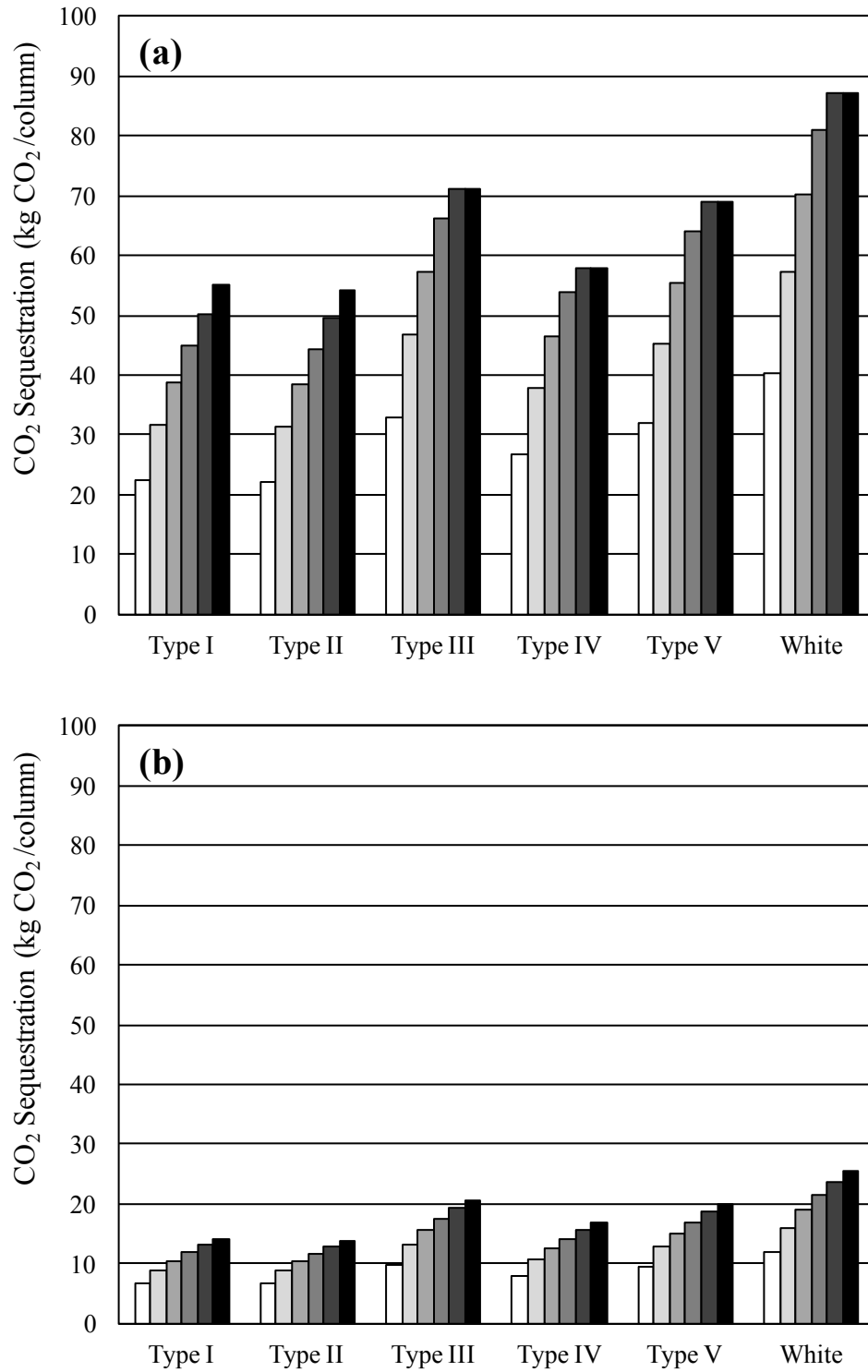


Figure 1 Effect of cement type on carbon sequestration potential in (a) XC1 high- (800 ppm) and (b) XC4 low- concentration (300 ppm) CO₂ environments after 25 (○), 50 (◐), 75 (◑), 100 (◒), 125 (◓), and 150 (◔) years of exposure for a 40 MPa concrete column (0.5 x 0.5 x 3m).

The diminishing effect of total sequestered CO₂ with time is demonstrated by all cement types in both CO₂ environments. Type I and White cement concrete columns sequester 22.4 kg CO₂ and 40.5 kg CO₂, respectively, for this application after the first 25 years of exposure in a XC1 high-concentration CO₂ environment. These columns only sequester an additional 32.5 kg CO₂ and 46.8 kg CO₂, respectively, after 125 years of further exposure (150 years). This reduction in the rate of CO₂ sequestration is attributable to the time-dependent decay in total carbonation depth (Eq. 11).

Figure 1a also demonstrates that the total volume of this particular concrete column can carbonize in its entirety while exposed in-service to a XC1 high CO₂ concentration environment. For example, Type III, IV, V and White cement concrete columns reach their maximum theoretical carbon sequestration potential after 125 years of exposure. The theoretical maximum for a Type IV cement, 40 MPa concrete column is 58 kg CO₂, while, for a White cement, 40 MPa concrete column of identical volume, an additional 50% can be sequestered (87 kg total). These results demonstrate that reaching the theoretical carbon sequestration potential during service depends not only on exposure conditions, but also on cement composition.

4.1.3 Effect of concrete compressive strength

To elucidate the effects of concrete compressive strength, sample concrete mixtures of varying 28-day compressive strengths were designed according to the Portland Cement Association concrete mixture design methodology [Kostmaka 2002]. In order to calculate cement content, each concrete mixture was initially designed using a Type I ASTM C 150 cement with a relative density of 3.15, maximum coarse aggregate size of 2 cm with an oven-dry relative density of

2.68 (ATM C 33), natural sand with an oven-dry relative density of 2.64 (ASTM C33), an air-entraining mixture of wood-resin type (ASTM C 260), and 7% air content. The resulting sample mixtures are shown below in Table 6.

Table 6 Sample mixture proportions (kg/m³) for concretes of varying compressive strengths.

Concrete Mixture Constituents	Concrete Design Compressive Strength				
	15 MPa	25 MPa	30 MPa	40 MPa	45 MPa
Cement	281	381	451	572	641
Water	102	106	110	115	118
Coarse Aggregate	1013	1013	1013	1013	1013
Fine Aggregate	866	1310	715	698	547

Similar to the effects of cement type, compressive strength, which is highly governed by cement (and water) content, directly influences both in-service and total carbon sequestration potential. Figure 2 illustrates the effect of design compressive strength on the carbon sequestration potential of a Type I cement concrete mixture (see Table 7) for a 0.5 x 0.5 x 3 m column ($SA/V = 8 \text{ m}^{-1}$) after 25, 50, 75, 100, 125 and 150 years of exposure in both an indoor (XC1) a high-concentration (800 ppm) (Figure 2a) and outdoor (XC4) low-concentration (300 ppm) CO₂ environment (Figure 2b).

Again, as anticipated, the theoretical sequesterable CO₂, in general, increases with time and with favorable exposure conditions for each concrete mixture. A Type I, 40 MPa concrete column, for example, exhibits a 145% increase in sequesterable CO₂ between 25 and 150 years in a XC1 environment (Figure 2a). A 290% increase is observed for the same Type I, 40 MPa concrete column in a XC1 versus XC4 environment after 150 years of exposure. Similar time- and

concentration-dependent behavior is exhibited by all mixture formulations except the Type I 15 MPa, 25 MPa, and 30 MPa concrete columns, which, as illustrated by the plateaus in the data (Figure 2a), reach the theoretical carbon sequestration limit in a XC1 high-concentration CO₂ environment after 25, 75, and 125 years of exposure, respectively.

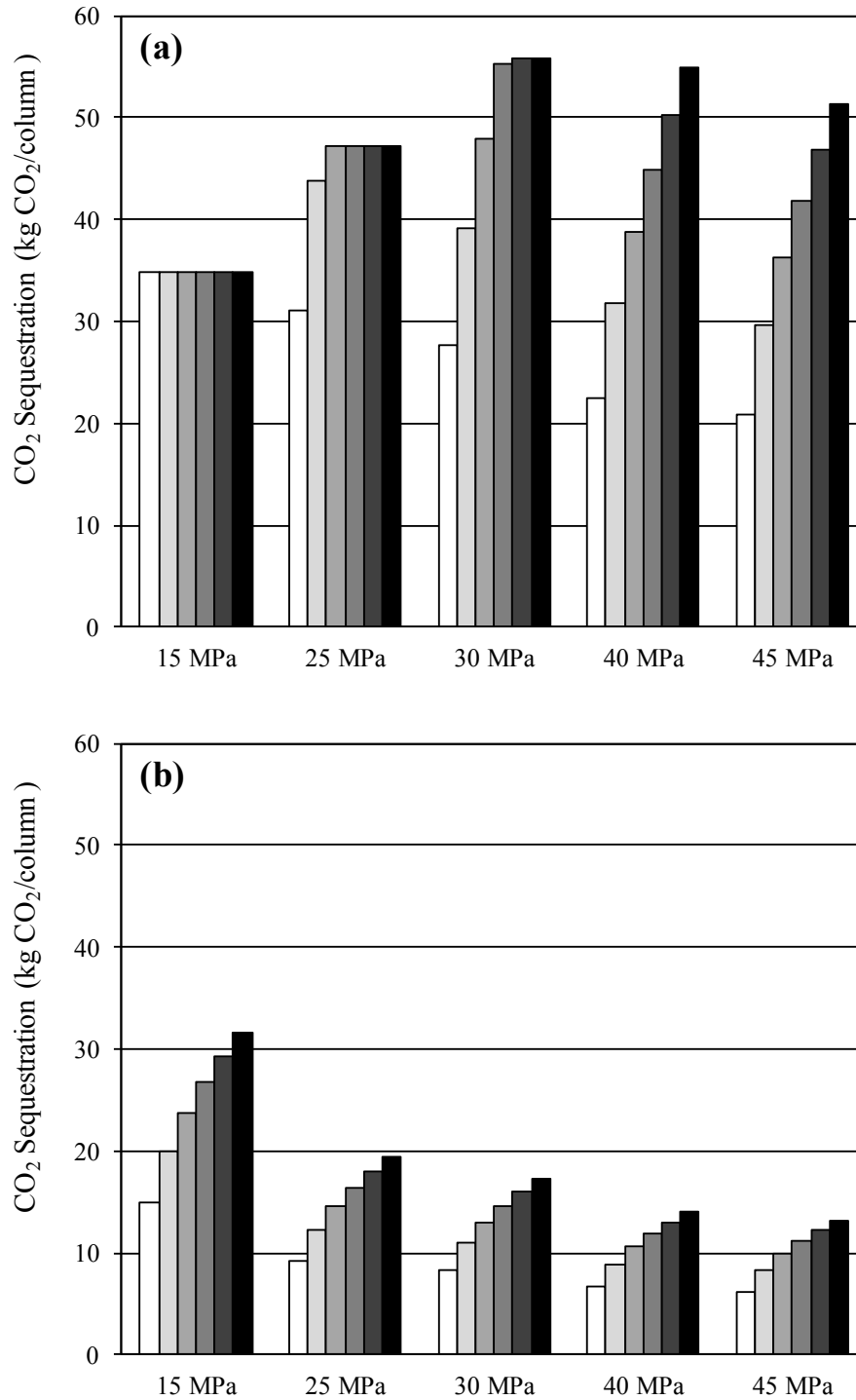


Figure 2 Effect of compressive strength on carbon sequestration potential in (a) XC1 high- (800 ppm) and (b) XC4 low-concentration (300 ppm) CO₂ environments after 25 (○), 50 (◐), 75 (◑), 100 (◒), 125 (◓), and 150 (◔) years of exposure for a Type I cement concrete.

Figure 2b also demonstrates that, in general, an increase in compressive strength correlates to reductions in total sequesterable CO₂ at early ages (25-50 years). This trend is also observable for the non-plateaued data for the 40 MPa and 50 MPa columns in Figure 2a. However, the theoretical limit of total sequesterable CO₂ is, in fact, maximized in high-compressive strength concretes as the total carbonated volume approaches the total concrete volume ($V_c \rightarrow V$) as $t \rightarrow \infty$, which is suggested by the plateaued data in Figure 2a for the 15 MPa, 25 MPa, and 30 MPa columns. Increased compressive strengths require higher cement contents (see Table 6), thus increasing the theoretical potential for CO₂ sequestration (Eq. 15). However, the carbonation resistance factor, R , also increases with compressive strength (Eq. 12). This increase is attributable to denser microstructures and lower overall gas and liquid permeabilities that result from high-strength concrete mixtures. In sum, the data show that lower compressive strengths, high CO₂ exposure, and time increase the total sequesterable CO₂ at early ages. However, this time- and exposure-dependent reduction is overcome at later ages. To illustrate, a Type I 25 MPa concrete column sequesters 31.0 kg CO₂, while a Type I 45 MPa concrete sequesters 21.0 kg CO₂ after 25 years in a XC1 high-concentration (800 ppm) CO₂ environment. The theoretical carbon sequestration limits for the Type I 25 MPa and Type I 45 MPa concrete columns (as $t \rightarrow \infty$), however, are 47.2 kg CO₂ and 59.2 kg CO₂ (data not shown), respectively.

While these data were specific for a Type I cement concrete, the effect of cement type, compressive strength, and time on carbon sequestration potential of a concrete column with equal dimensions in a XC1 high-concentration (800 ppm) CO₂ environment is illustrated in Figure 3.

These results show that more CO₂ is sequestered (1) in lower-strength concretes at early ages, (2) in higher-strength concretes at later ages, and (3) in concretes with low-C₄AF cements (i.e., Type III, Type V, White). For instance, after 25 years of exposure, a Type I, 15 MPa concrete column sequesters 66% more CO₂ than a Type I, 45 MPa concrete column. After 150 years, however, the Type I, 45 MPa concrete sequesters 47% more CO₂ than the Type I, 15 MPa concrete column (Figure 3a). Furthermore, a low-C₄AF White cement 45 MPa concrete, sequesters 83% more CO₂ than the Type I, 45 MPa concrete after 150 years. All concrete specimens demonstrate that approximately 40% of all carbon sequestration occurs within the first 25 years of exposure. Additionally, for low-strength concrete columns with, hence, a lower carbonation resistance factor, R, the theoretical maximum carbonation is reached after 50 years of exposure for this column geometry, as noted by the 15 MPa concrete plateau effect in Figures 3a-3f.

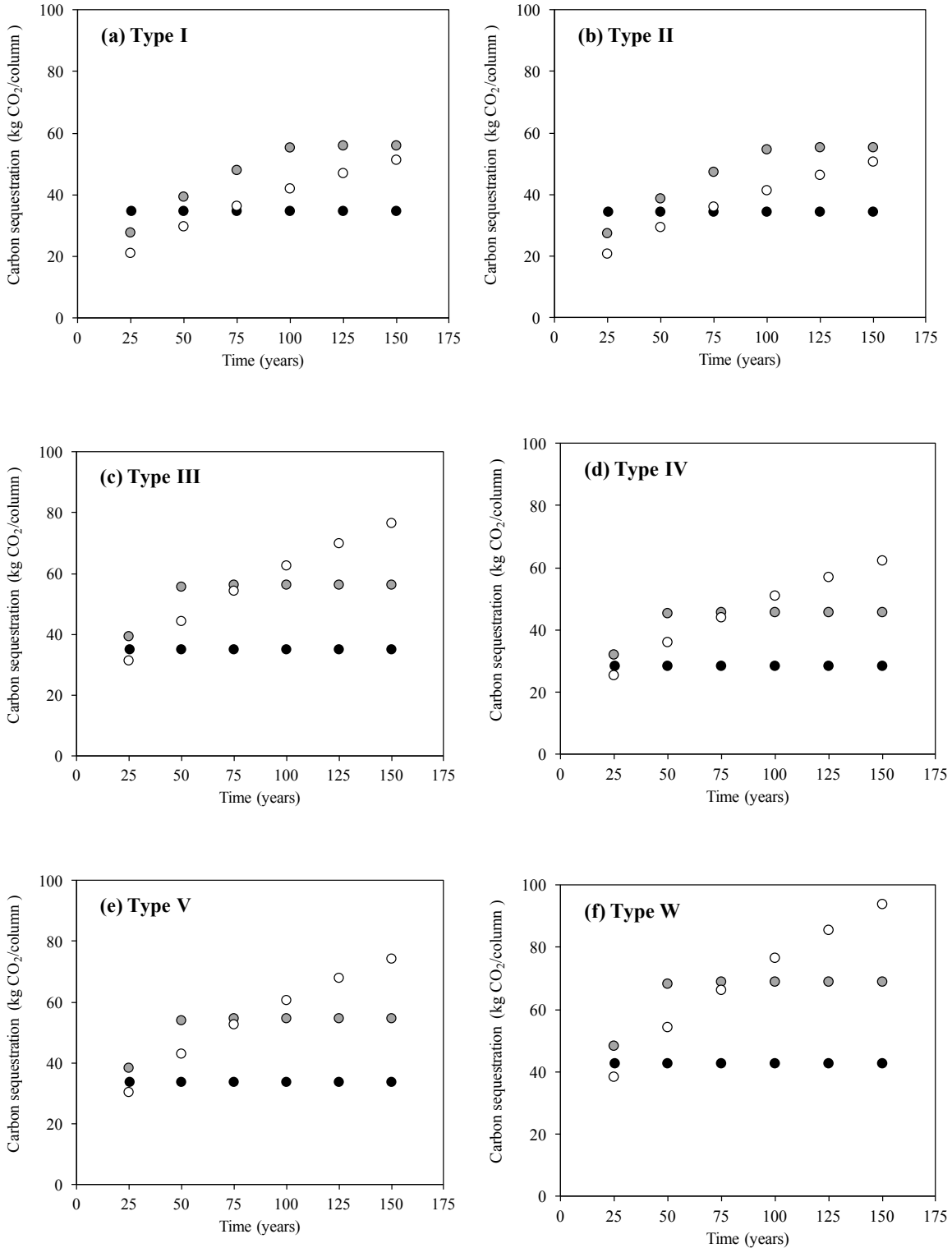


Figure 3 Effect of cement type, namely (a) Type I, (b) Type II, (c) Type III, (d) Type IV, (e) Type V, and (f) White, and time on the carbon sequestration potential of 15 MPa (●), 30 MPa (●), and 45 MPa (○) compressive strength concrete columns (0.5 x 0.5 x 3 m).

4.1.4 Effect of SCMs

Figure 4 illustrates the anticipated percent reduction in carbon sequestration potential, C_m (kg CO₂/kg cement) per type and amount of SCM. The data shown in Figure 4 are independent of cement type and total cement content in the concrete mixtures. Expectedly, increased reductions in CO₂ sequestration are observed with increased weight-percent replacement of silica-rich SCMs. As previously discussed, when OPC is partially replaced by SCMs, the pozzolanic nature of siliceous SCM minerals react with CH, rendering less CH available for CO₂ sequestration. In addition, the reduction in CO₂ sequestration potential depends on the type of SCM (i.e., Class F fly ash, Class C fly ash, silica fume, slag, metakaolin).

As anticipated, silica fume, the most silica-rich of all SCMs, demonstrates the greatest reduction in CO₂ sequestration potential, while Class C fly ash demonstrates the least reduction per weight-percent cement replacement. To achieve a 60% reduction in CO₂ sequestration potential, for example, would require only 10% replacement of cement with silica fume versus a 46% replacement with Class C fly ash. Class F fly ash and metakaolin demonstrate identical reductions in CO₂ sequestration potential due to similar silica contents on a per mass basis, which is represented by the β factor presented in Table 2.

The data in Figure 4 also show upper-bound limits to pozzolanic reactivity per SCM, which coincides with an elimination of any potential for carbon sequestration. For example, if cement were replaced with silica fume, Class F fly ash (or metakaolin), slag, or Class C fly ash by more than 15%, 30%, 44%, and 60%, respectively, theoretically no CO₂ sequestration would be expected according to this model.

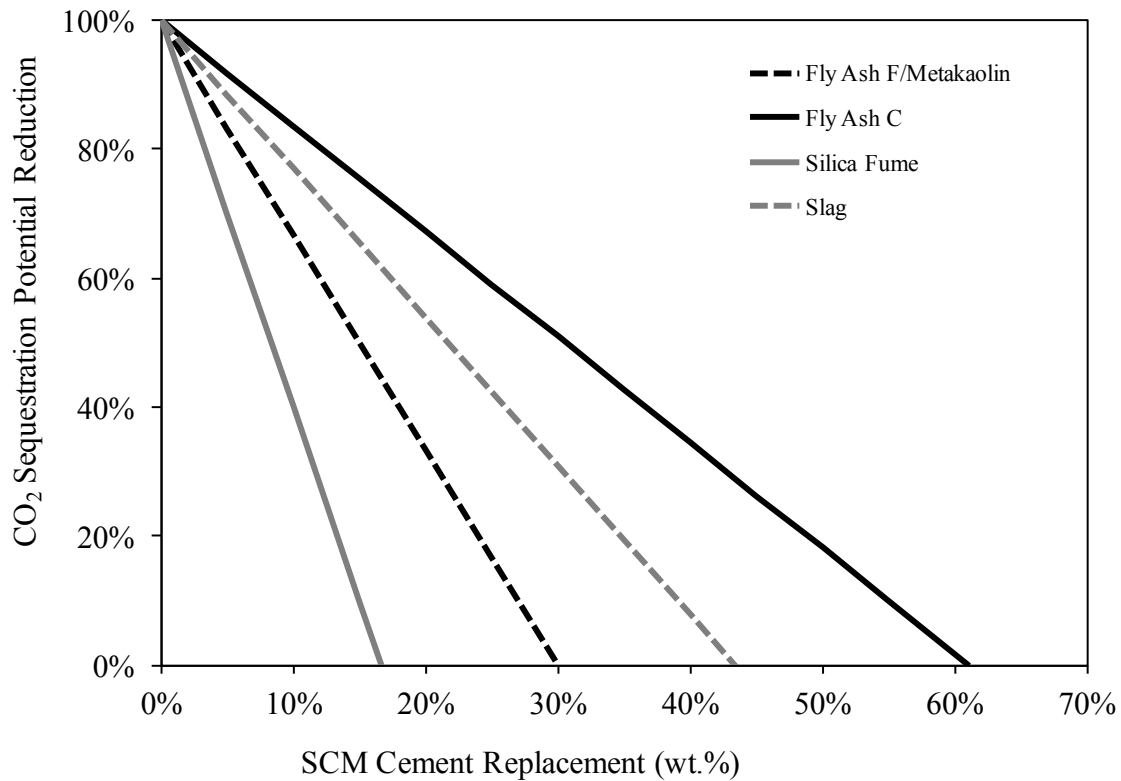


Figure 4 Anticipated reductions in carbon sequestration potential, C_m , per SCM type and weight-percent cement replacement. Data shown are valid for all cement types (Type I-V, White).

4.1.5 Effect of environmental exposure

CO_2 concentration depends on exposure classification. An XC1 exposure is used, for example, for cases where reinforced concrete is located inside buildings or structures, where the CO_2 concentration in that location is high in comparison to a XC4 exposure, where outer surfaces of concrete elements are exposed to the outdoors. On average, indoor concentrations are approximately 700 ppm above normal outdoor CO_2 concentrations, which range between 300-500 ppm [Rudnick 2003]. For the purposes of this study, the assumed placement of elements

(indoor vs. outdoor) is linked to XC1 and XC4 exposure classification and to CO₂ concentrations of 800 ppm (1.55×10^{-3} kg/m³) and 300 ppm (0.581×10^{-3} kg/m³), respectively.

The effect of CO₂ concentration (ppm), exposure classification (i.e., XC1, XC2, XC3, XC4), and cement type on the carbon sequestration of a 40 MPa concrete column (0.5 x 0.5 x 3 m) after 100 years of exposure is shown in Figure 5. Expectedly, an increase in CO₂ concentration (ppm) resulted in higher in-situ CO₂ sequestration for all exposure classifications and cement types. A surface-exposed column placed indoors, for example, (XC1) with a high concentration of CO₂ (2000 ppm) absorbs 216% more CO₂ after 100 years than if it were exposed to lower concentrations (200 ppm). This finding suggests that elevated levels of CO₂ may be beneficial to promote in-situ CO₂ sequestration in an indoor environment.

Results in Figure 5 also demonstrate the influence of exposure classification on in-service carbon sequestration potential. For example, an exposed-surface column inside a building (XC1) will absorb a higher amount of CO₂ than concrete columns submerged in soil or water (XC2), encased and protected from ambient conditions (XC3), or exposed to wetting/drying cycles or rain (XC4). A 40 MPa White cement concrete column in XC1 exposed to a high concentration (1000 ppm) of CO₂, for example, sequesters 121% more CO₂ after 100 years than the same column located in XC4 at the same CO₂ concentration. In instances where concrete surfaces are not exposed to the surrounding environment (XC2), in-service carbon sequestration potential is reduced. The same 40 MPa White cement concrete column that is surface-exposed inside a building (XC1) to a low-CO₂ concentration environment (400 ppm) absorbs 372% more CO₂ than a column that is not exposed (XC2) at the same CO₂ concentration after 100 years. In

summary, the data in Figure 5 further suggest that in-situ CO₂ sequestration is maximized in low-C₄AF cement (Type III, V, White) concretes, as previously elucidated in Section 3.1, and in elements that are surface-exposed to high-CO₂ concentrations in indoor environments. Such findings can be leveraged to inform and maximize the benefit of carbon-capture and carbon-storage strategies in low-carbon building.

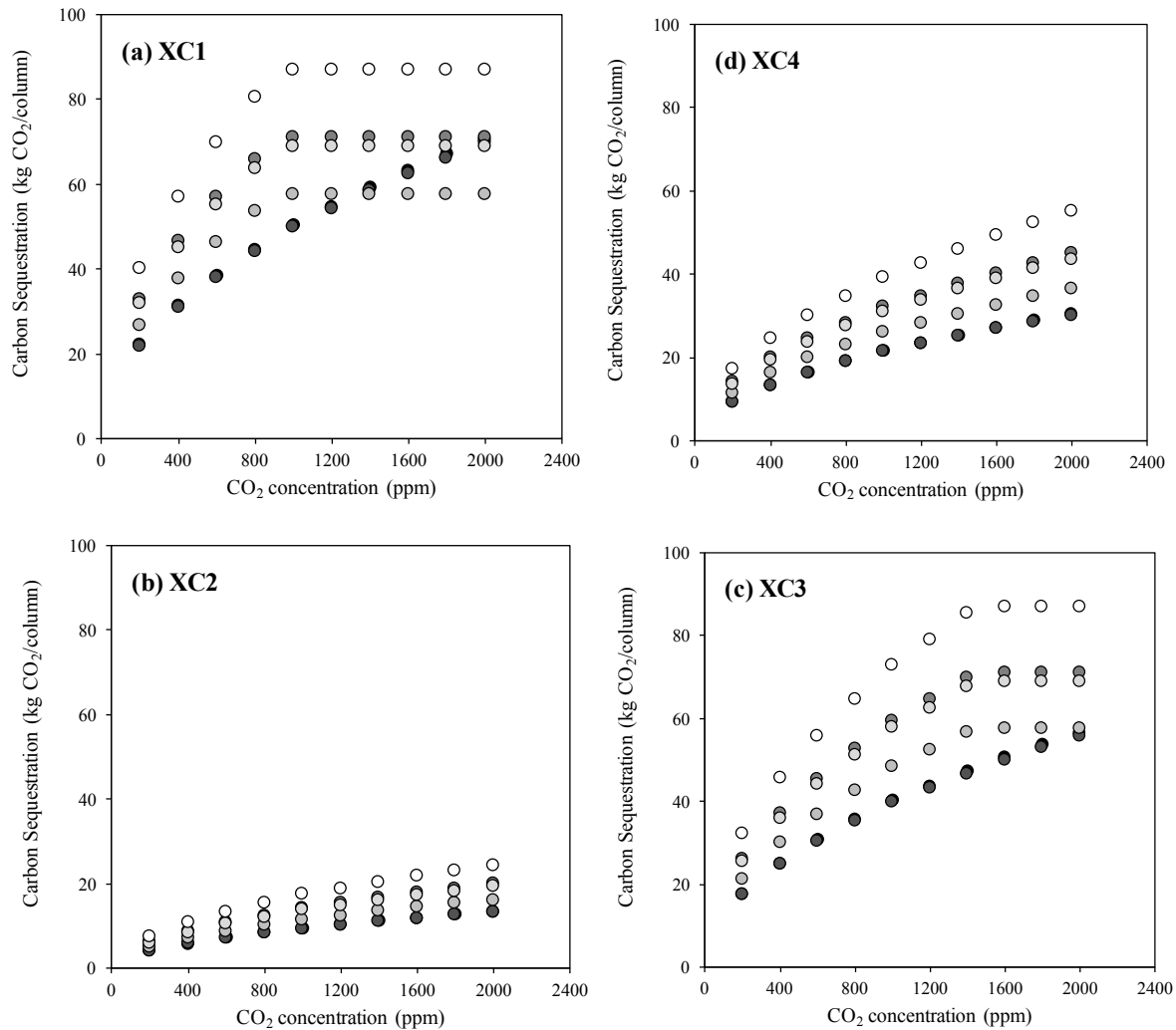
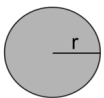
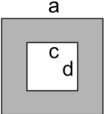
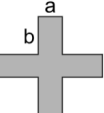


Figure 5 Effect of CO₂ concentration and exposure environment, namely (a) XC1, (b) XC2, (c) XC3, and (d) XC4, on the carbon sequestration of a 40 MPa Type I (●), Type II (●), Type III (●), Type IV (●), Type V (●), and White (○) cement concrete columns (0.5 x 0.5 x 3 m).

4.1.6 Effect of structural geometry

Given that the carbonation process is a surface-dominated, rate-dependent phenomenon, the total amount of sequesterable CO₂ per unit of time is related to the carbonation depth and total exposed surface area in direct contact with air or water. For this reason, the geometry, namely the surface area, SA, and total volume, V, of concrete elements will directly influence total CO₂ sequestration. To investigate the effect of surface-area-to-volume (SA/V) ratio on CO₂ sequestration potential, several cross-sectional geometries of concrete columns were considered. The cross-sectional area (0.25 m²), length (3 m), and volume (0.75 m³) of each column were held constant. Table 7 illustrates the shape, cross-sectional dimensions, total surface area, and SA/V ratios of the concrete columns considered herein.

Table 7 Column geometries considered in analyzing the effect of SA/V on carbon sequestration potential. Each column had a fixed cross-sectional area, length, and volume.

Cross-Section	Geometry	Dimensions (m)	Total Surface Area (m ²)	SA/V Ratio (m ⁻¹)
1		r = 0.28	5.3	7.1
2		a = 0.5 b = 0.5	6.0	8.0
3		a = 0.6 b = 0.6 c = 0.33 d = 0.33	11.2	14.9
4		a = 0.14 b = 0.4	11.3	15.1
5		a = 0.1 b = 2.4	15.0	20.0

In recognition that carbonation and, thus, carbon sequestration of concrete elements is a surface-dominated phenomenon, Figure 6 illustrates the effect of structural geometry, namely SA/V ratio of Type I, 40 MPa concrete columns with varying cross-sectional dimensions presented in Table 7, and length of exposure on CO₂ sequestration potential in both an indoor (XC1) high-concentration (800 ppm) CO₂ (Figure 6a) and an outdoor (XC4) low-concentration (300 ppm) CO₂ (Figure 6b) environment.

The data in both Figure 6a and Figure 6b demonstrate that higher SA/V ratios result in higher amounts of sequestered carbon at all ages of in-service exposure. For instance, a cross-shaped column section (SA/V=15.1 m⁻¹) will absorb 198% more CO₂ than a traditional cylindrical column of the same volume (SA/V=7 m⁻¹). Therefore, if the geometries of all 25 columns in a medium-size office building that were exposed to the interior (800 ppm) were altered to increase the SA/V ratio from 7 m⁻¹ to 15 m⁻¹, an additional 110% (795 kg) CO₂ could be sequestered after 50 years. If, for example, the geometries were changed from cylindrical to swirl-shaped (SA/V=20 m⁻¹), after 25 years of exposure in the same high-concentration CO₂ environment, the 25 columns in the building could sequester 185% (910 kg) more CO₂. Percent increases are identical in either a high- or low-concentration CO₂ environment, rendering the SA/V-related increases in carbon sequestration potential independent of environmental exposure.

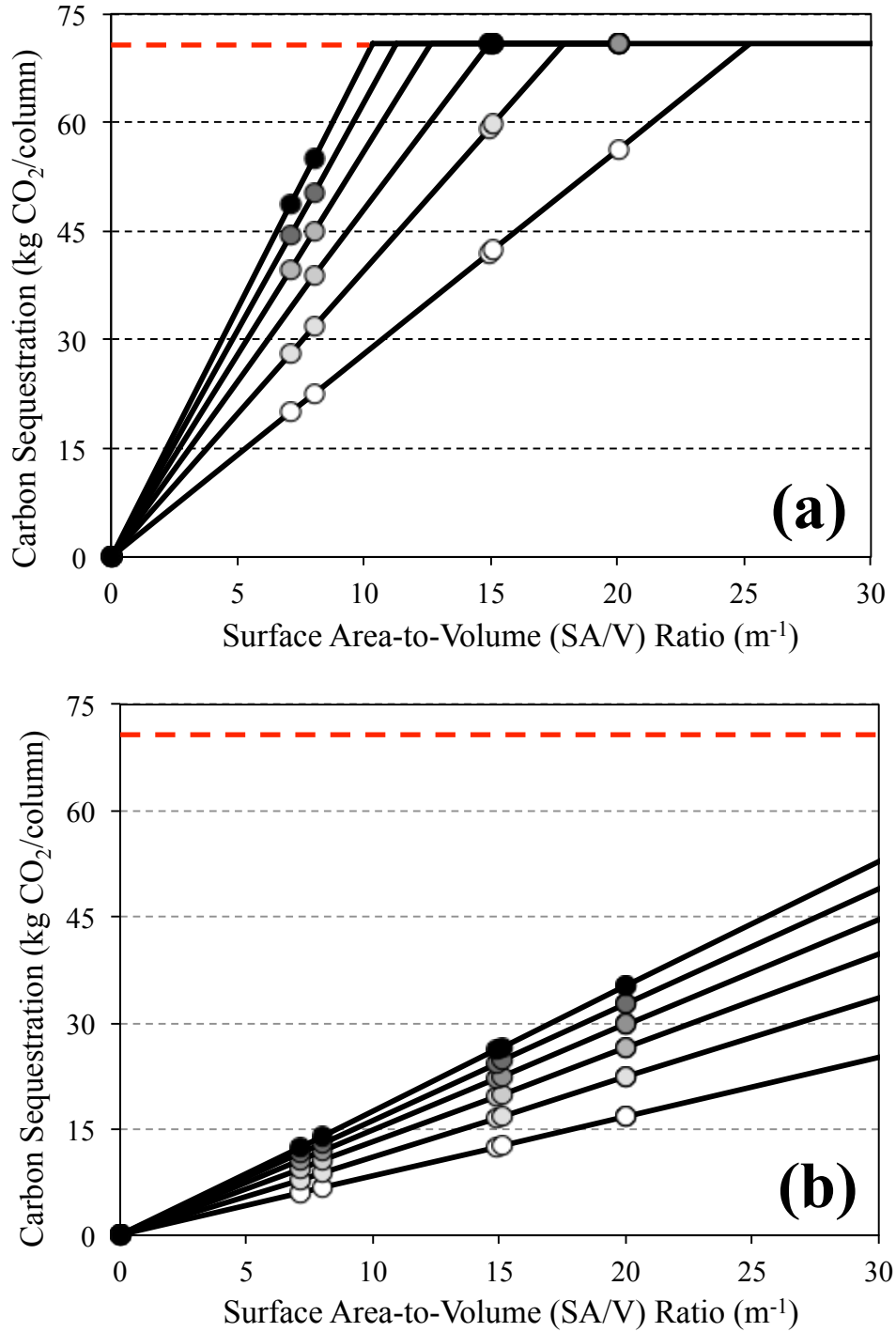


Figure 6 Influence of SA/V ratio on sequesterable CO₂ for Type I, 40 MPa structural concrete columns ($V = 0.75 \text{ m}^3$) in (a) high- (800 ppm) and (b) low-concentration (300 ppm) CO₂ environments after 25 (○), 50 (◐), 75 (◑), 100 (◒), 125 (◓), and 150 (◔) years. Theoretical limit (---) assumes a service life, $t = \infty$.

Figure 6 also illustrates that, while higher SA/V ratios result in higher amounts of sequestered carbon at all finite ages of exposure, all shapes will eventually reach the theoretical limit of 70.8 kg CO₂ at infinite ages for this particular volume ($V=0.75\text{m}^3$) of Type I, 40 MPa concrete. In this analysis, a 100% carbonation degree has been assumed, thus concrete elements with high SA/V ratio ($SA/V>15\text{ m}^{-1}$) located in high CO₂ concentration environments can reach this theoretical limit after 75-100 years. However, realistic volumes of concrete elements will not likely reach theoretical limits while in service. Practically, concrete structures would likely reach theoretical limit post-deconstruction, when concrete elements are demolished and crushed into high surface-area rubble. In this case, concrete may experience accelerated carbonation and, depending upon post-deconstruction exposure conditions, could reach the theoretical limit prescribed by the model proposed herein. When incorporating this particular model into WBLCA, the estimated CO₂ sequestered will vary depending on the chosen system boundary. For instance, in a cradle-to-cradle study, where the effects of post-use crushing and recycling concrete are included, it can be immediately assumed that the volume carbonated will be equivalent to the total volume of the concrete element (i.e., $t = \infty$). However, in cases where the system boundary of interest does not include end-of-life exposure (i.e., $t \neq \infty$), the carbon sequestration benefits of post-use carbon sequestration are not included in the model prediction.

The magnitude of carbon sequestration in relation to initial carbon emissions is highly dependent upon the cradle-to-gate lifecycle assessment of the OPC concrete element. Recent studies have shown that certain concrete elements can sequester anywhere from 15 to 17% of initial CO₂ emissions [27] or up to 41% [26]. The results from this study indicate that the degree of recarbonation of any structural element will be highly dependent not only on the initial carbon

emissions during manufacture, transport, and construction, but also on the type and amount of cement, SCMs, compressive strength, and geometry of the individual concrete element.

It is evident from the data that, for the same volume of concrete, high SA/V-ratio geometries are preferred in terms of carbon sequestration potential in situations where the service life of the structure is predicted to be less than 50 years. In order to achieve higher SA/V ratios, however, complex structural shapes are required. Circular and square cross-sections, which exhibit the lowest SA/V ratios, currently dominate for fast, low-cost construction. However, more complex structural shapes could be made possible by emerging technologies, such as additive manufacturing (3D printing).

Finally, Figure 6 illustrates that high CO₂ environments enhance in-situ CO₂ sequestration, which, in concert with findings presented in previous sections, indicates that a combination of (1) innovations in structural geometries (high SA/V ratios), (2) high CO₂ exposure, (3) low-C₄AF cements, (4) no SCMs, (5) low-compressive strengths at early ages, (6) high-compressive strengths at later ages, and (7) interior placement would be most favorable in order to strategically maximize the in-service CO₂ sequestration potential of exposed reinforced concrete elements.

CHAPTER 5

CONCLUSIONS

A simple model for predicting the carbon sequestration potential of exposed ordinary portland cement (OPC) concrete elements was formulated and implemented in this work. The model, which is based on OPC cement hydration and carbonation reaction chemistry, accounts for type and quantity of cements and weight-percent replacement of cement by supplementary cementitious materials (SCMs). The effects of each of these parameters on the theoretical carbon dioxide (CO₂) sequestration of OPC concrete elements were investigated for a variety of CO₂ environmental exposure classifications. In addition, the influence of concrete design compressive strength and structural geometry, namely the effect of increasing surface-area-to-volume (SA/V) ratio of exposed concrete elements, on sequesterable CO₂ was investigated herein.

As anticipated, the results confirm that total sequesterable CO₂ increases not only with exposure time, but also with CO₂ concentration while in service. In addition, White cement exhibited the highest CO₂ sequestration potential of all cement types, due to its low C₄AF content. Results also suggest that low-strength concretes sequester more CO₂ at early ages, but high-strength concretes sequester more CO₂ at later ages, elucidating a time-dependent influence of compressive strength on total carbon sequestration.

The data illustrate that, when OPC is partially replaced by SCMs, the CO₂ sequestration potential is reduced and that this reduction depends upon type of SCM and weight-percent cement replacement. Silica-rich SCMs, such as silica fume, Class F fly ash, and metakaolin, exhibit the most reductions in CO₂ sequestration potential per weight-percent replacement compared to

SCMs with lower silica contents (e.g., slag, Class C fly ash). Furthermore, the amount of sequesterable CO₂ depends on the exposure classification of the OPC concrete element. CO₂ sequestration was enhanced in permanently dry or humid conditions and reduced in cyclically humid and dry conditions, suggesting that it is favorable to place OPC concrete elements inside the building envelope rather than outside to maximize in-situ sequestration.

Innovative structural geometries, namely increasing the SA/V ratios of concrete elements, can enhance the carbon sequestration potential of OPC concrete structures. By analyzing columns of similar volumes but with varying surface-area geometries, it was found that total, in-situ sequesterable CO₂ can be enhanced by up to 255% compared to round, cylindrical columns. Innovative geometries required for high-SA/V ratio structural elements are increasingly achievable with advancements in additive manufacturing construction technologies.

The model presented herein can be employed to quantify carbon sequestration potential of reinforced OPC concrete elements when implementing a whole-building lifecycle assessment (WBLCA). Total sequesterable carbon can be calculated for concrete elements while in service (assuming a finite lifetime) or out of service (assuming an infinite lifetime). As discussed, the model presented in this paper is notably conservative, since it does not account for participation by other ferritic or calcium-containing compounds (i.e., CSH) in the carbon sequestration process.

In summary, the findings suggest that novel materials design considerations (low C₄AF cement, low compressive strength, no SCMs), structural concrete design innovations (high SA/V ratio),

and new air quality strategies (minimum ppm CO₂) could be implemented to maximize in situ sequestration via exposure of OPC concrete elements to CO₂-rich environments. Given that enhanced carbonation during service may lead to premature serviceability concerns with carbonation-induced corrosion of mild steel reinforcement, design decisions related to maximizing carbon sequestration potential of exposed OPC concrete should be made within a more holistic lifecycle sustainability context.

REFERENCES

American Society of Testing and Materials (ASTM), Standard specification for Portland cement, West Conshohocken, PA USA, 2016.

Ashraf, W. (2016). Carbonation of cement-based materials: Challenges and opportunities. *Construction and Building Materials*, 120, 558-570.

Asif, M., Muneer, T., & Kelley, R. (2007). Life cycle assessment: a case study of a dwelling home in Scotland. *Building and environment*, 42(3), 1391-1394.

Barnett, C. L. (2007). *Green Buildings: Benefits to Health, the Environment, and the Bottom Line*. US Senate Environment and Public Works Committee Hearing, Washington, DC, May 15, 2007. Healthy Schools Network, Inc.

Basbagill, J., Flager, F., Lepech, M., & Fischer, M. (2013). Application of life-cycle assessment to early stage building design for reduced embodied environmental impacts. *Building and Environment*, 60, 81-92.

Berndt, M. L. (2009). Properties of sustainable concrete containing fly ash, slag and recycled concrete aggregate. *Construction and building materials*, 23(7), 2606-2613.

Bribián, I. Z., Usón, A. A., & Scarpellini, S. (2009). Life cycle assessment in buildings: State-of-the-art and simplified LCA methodology as a complement for building certification. *Building and Environment*, 44(12), 2510-2520.

Collins, F. (2010). Inclusion of carbonation during the life cycle of built and recycled concrete: influence on their carbon footprint. *The International Journal of Life Cycle Assessment*, 15(6), 549-556.

Crow, J. M. (2008). The concrete conundrum. *Chemistry World*, 5(3), 62-66.

Damtoft, J. S., Lukasik, J., Herfort, D., Sorrentino, D., & Gartner, E. M. (2008). Sustainable development and climate change initiatives. *Cement and concrete research*, 38(2), 115-127.

Engelsen, C.J., Justnes, H. (2014) CO₂ binding by concrete. A summary of the state of the art and an assessment of the total binding in by carbonation in the Norwegian concrete stock. SINTEF Building and Infrastructure, Construction Technology, Norway.

Fridh, K., Lagerblad, B. (2013) Carbonation of indoor concrete: Measurements of depths and degrees of carbonation. (Report TVBM; Vol. 3169). Division of Building Materials, LTH, Lund University.

Galan, I., Andrade, C., Mora, P., & Sanjuan, M. A. (2010). Sequestration of CO₂ by concrete carbonation. *Environmental science & technology*, 44(8), 3181-3186.

García-Segura, T., Yepes, V., Martí, J. V., & Alcalá, J. (2014). Optimization of concrete I-beams using a new hybrid glowworm swarm algorithm. *Latin American Journal of Solids and Structures*, 11(7), 1190-1205.

García-Segura, T., Yepes, V., & Alcalá, J. (2014). Life cycle greenhouse gas emissions of blended cement concrete including carbonation and durability. *The International Journal of Life Cycle Assessment*, 19(1), 3-12.

Haapio, A., & Viitaniemi, P. (2008). A critical review of building environmental assessment tools. *Environmental impact assessment review*, 28(7), 469-482.

Huntzinger, D. N., & Eatmon, T. D. (2009). A life-cycle assessment of Portland cement manufacturing: comparing the traditional process with alternative technologies. *Journal of Cleaner Production*, 17(7), 668-675.

Jiang, L., Lin, B., & Cai, Y. (2000). A model for predicting carbonation of high-volume fly ash concrete. *Cement and Concrete Research*, 30(5), 699-702.

Johannesson, B., & Utgenannt, P. (2001). Microstructural changes caused by carbonation of cement mortar. *Cement and concrete Research*, 31(6), 925-931.

Junnila, S., & Horvath, A. (2003). Life-cycle environmental effects of an office building. *Journal of Infrastructure Systems*, 9(4), 157-166.

Kashef-Haghighi, S., Shao, Y., & Ghoshal, S. (2015). Mathematical modeling of CO₂ uptake by concrete during accelerated carbonation curing. *Cement and Concrete Research*, 67, 1-10.

Khasreen, M. M., Banfill, P. F., & Menzies, G. F. (2009). Life-cycle assessment and the environmental impact of buildings: a review. *Sustainability*, 1(3), 674-701.

Knoeri, C., Sanyé-Mengual, E., & Althaus, H. J. (2013). Comparative LCA of recycled and conventional concrete for structural applications. *The International Journal of Life Cycle Assessment*, 18(5), 909-918.

Kosmatka, S. H., Panarese, W. C., & Kerkhoff, B. (2002). Design and control of concrete mixtures (Vol. 5420, pp. 60077-1083). Skokie, IL: Portland Cement Association.

Lagerblad, B., (2006). Carbon Dioxide Uptake During Concrete Life Cycle - State of the Art, Swedish Cement and Concrete Research Institute

Lee, S., Park, W., & Lee, H. (2013). Life cycle CO₂ assessment method for concrete using CO₂ balance and suggestion to decrease LCCO₂ of concrete in South-Korean apartment. *Energy and Buildings*, 58, 93-102.

Malhotra, V. M. (1999). Role of supplementary cementing materials in reducing greenhouse gas emissions. In *Infrastructure regeneration and rehabilitation improving the quality of life through better construction*. International conference (pp. 27-42).

Marinković, S., Radonjanin, V., Malešev, M., & Ignjatović, I. (2010). Comparative environmental assessment of natural and recycled aggregate concrete. *Waste Management*, 30(11), 2255-2264.

Mehta, K. P. (2001). Reducing the environmental impact of concrete. *Concrete international*, 23(10), 61-66.

Monteiro, I., Branco, F. A., De Brito, J., & Neves, R. (2012). Statistical analysis of the carbonation coefficient in open air concrete structures. *Construction and Building Materials*, 29, 263-269.

Mounanga, P., Khelidj, A., Loukili, A., & Baroghel-Bouny, V. (2004). Predicting Ca (OH) 2 content and chemical shrinkage of hydrating cement pastes using analytical approach. *Cement and Concrete Research*, 34(2), 255-265.

Nilsson, L. O. (2011). A new model for CO₂-absorption of concrete structures. Lund Institute of Technology, Report TVBM, 3158.

Nishikawa, T., Suzuki, K., Ito, S., Sato, K., & Takebe, T. (1992). Decomposition of synthesized ettringite by carbonation. *Cement and Concrete Research*, 22(1), 6-14.

Pade, C., & Guimaraes, M. (2007). The CO₂ uptake of concrete in a 100 year perspective. *Cement and Concrete Research*, 37(9), 1348-1356.

Papadakis, V. G., Vayenas, C. G., & Fardis, M. N. (1991). Experimental investigation and mathematical modeling of the concrete carbonation problem. *Chemical Engineering Science*, 46(5-6), 1333-1338.

Papadakis, V. G., Vayenas, C. G., & Fardis, M. N. (1991). Fundamental modeling and experimental investigation of concrete carbonation. *Materials Journal*, 88(4), 363-373.

Peter, M. A., Muntean, A., Meier, S. A., & Böhm, M. (2008). Competition of several carbonation reactions in concrete: A parametric study. *Cement and Concrete Research*, 38(12), 1385-1393.

Peuportier, B. L. P. (2001). Life cycle assessment applied to the comparative evaluation of single family houses in the French context. *Energy and buildings*, 33(5), 443-450.

Pommer, K., & Pade, C. (2006). Guidelines: Uptake of carbon dioxide in the life cycle inventory of concrete (pp. 1-82). Nordic Innovation Centre.

Ramesh, T., Prakash, R., & Shukla, K. K. (2010). Life cycle energy analysis of buildings: An overview. *Energy and buildings*, 42(10), 1592-1600.

Roy, S. K., Poh, K. B., & Northwood, D. O. (1999). Durability of concrete—accelerated carbonation and weathering studies. *Building and environment*, 34(5), 597-606.

Rudnick, S. N., & Milton, D. K. (2003). Risk of indoor airborne infection transmission estimated from carbon dioxide concentration. *Indoor air*, 13(3), 237-245.

Simonen, K. (2014) "Life Cycle Assessment." *Pocket Architecture: Technical Design Series*.

Srubar III, WV. (2014) "Beyond LCAs and EPDs: Importance of Service-Life Prediction for Green Materials and Structures." *Proceedings of the Sustainable Structures Symposium*; Portland, Oregon, USA.

Steffens, A., Dinkler, D., & Ahrens, H. (2002). Modeling carbonation for corrosion risk prediction of concrete structures. *Cement and Concrete Research*, 32(6), 935-941.

Thiery, M., Dangla, P., Belin, P., Habert, G., & Roussel, N. (2013). Carbonation kinetics of a bed of recycled concrete aggregates: a laboratory study on model materials. *Cement and Concrete Research*, 46, 50-65.

Torgal, F. P., Miraldo, S., Labrincha, J. A., & De Brito, J. (2012). An overview on concrete carbonation in the context of eco-efficient construction: Evaluation, use of SCMs and/or RAC. *Construction and Building Materials*, 36, 141-150.

Van Balen, K. (2005). Carbonation reaction of lime, kinetics at ambient temperature. *Cement and concrete research*, 35(4), 647-657.

Villain, G., & Thiery, M. (2006). Gammadensimetry: A method to determine drying and carbonation profiles in concrete. *NDT & E International*, 39(4), 328-337.

Wang, X. Y., & Lee, H. S. (2009). A model for predicting the carbonation depth of concrete containing low-calcium fly ash. *Construction and Building Materials*, 23(2), 725-733.

Yang, K. H., Seo, E. A., & Tae, S. H. (2014). Carbonation and CO₂ uptake of concrete. *Environmental Impact Assessment Review*, 46, 43-52.

Yang, K. H., Jung, Y. B., Cho, M. S., & Tae, S. H. (2015). Effect of supplementary cementitious materials on reduction of CO₂ emissions from concrete. *Journal of Cleaner Production*, 103, 774-783.

Yepes, V., Martí, J. V., & García-Segura, T. (2015). Cost and CO₂ emission optimization of precast–prestressed concrete U-beam road bridges by a hybrid glowworm swarm algorithm. *Automation in Construction*, 49, 123-134.

Worrell, E., Price, L., Martin, N., Hendriks, C., & Meida, L. O. (2001). Carbon dioxide emissions from the global cement industry 1. *Annual Review of Energy and the Environment*, 26(1), 303-329.